DOI: https://doi.org/10.2298/SARH220920085G
UDC: 616.71-006.3-07

ORIGINAL ARTICLE / ОРИГИНАЛНИ РАД

Can we distinguish conventional osteosarcoma subtypes (osteoblastic and chondroblastic) based on their magnetic resonnace signal intensities

Sabriye Gülçin Bozbeyoğlu[1], Ayse Nur Toksoz Yildirim[2]

[1]Istanbul Goztepe Prof. Dr. Suleyman Yalcin City Hospital, Department of Radiology, Istanbul, Turkey;
[2]Istanbul Goztepe Prof. Dr. Suleyman Yalcin City Hospital, Department of Pathology, Istanbul, Turkey

SUMMARY
Introduction/Objectives Osteosarcoma is the most common primary malignant bone tumor in adolescents and young adults, with a tendency to produce variable amounts of osteoid, cartilage, and fibrous matrices.
The objective of this study is to differentiate between osteosarcoma subtypes: osteoblastic and chondroblastic according to their magnetic resonance imaging (MRI) signal intensities and X-ray findings.
Methods We performed a retrospective analysis for 21 pathologically proven osteosarcoma subtypes: osteoblastic (n = 14) and chondroblastic (n = 7). Conventional images of the bone of origin, periosteal reactions, lytic and sclerotic features, the presence of calcification, and pathological fractures were investigated with X-rays. We measured the mean region of interest values for each lesion with MRI sequences.
Results Among the osteosarcoma lesions, 57% were localized at the knee. X-ray evaluations of the osteoblastic osteosarcomas revealed pure lytic lesions in 35.7%, and pure sclerotic lesions in 42.9% cases. Chondroblastic osteosarcomas revealed pure lytic lesions in 14.3% and pure sclerotic lesions in 42.9% cases. Due to variable osteoblastic, chondroblastic, and fibroblastic areas and proportions of the ossified matrix, osteosarcoma lesions have a heterogeneous MRI signal. However, no statistically significant value was detected.
Conclusion According to our results, MRI signal characteristics and X-ray findings may not be able to distinguish osteosarcoma subtypes, so prospective studies with larger patient cohorts are needed.
Keywords: magnetic resonance imaging; osteosarcoma; subtype; region of interest

INTRODUCTION

Osteosarcoma (OS) is the most common primary malignant bone tumor in adolescents and young adults, comprising 10% of solid cancers in patients between 15 and 19 years of age, with a tendency to produce variable amounts of osteoid, cartilage, and fibrous matrices. Although myeloma is the most common primary bone tumor in adults, OS also shows a second peak in adults in their 70s and 80s [1]. OS is classified according to the World Health Organization, with conventional high-grade central OS (HG-OS) as the most common subtype, accounting for 75–80% of all cases [2, 3]. Differentiating OS subtypes has clinical importance because of the differences in their prognosis and treatment [4].

Conventional OS are divided into three general subtypes: osteoblastic, chondroblastic, and fibroblastic. They all contain varying amounts of all three cell types in their matrices [5].

Radiographic assessment still has an unprecedented value in the initial assessment of HG-OS. The classic radiographic features include aggressive lytic bone destruction, osteoblastic matrix production, extraosseous soft tissue extension, and periosteal reactions [6]. These allow for a confident radiological diagnosis in the majority of cases as Figure 1. Other rare morphologic forms of conventional OS are giant cell-rich variants (numerous osteoclast-like giant cells), epithelioid variants, osteoblastoma-like variants, chondroblastoma-like variants, chondromyxoid fibroma-like OSs, clear cell variants, and small cell variants. Although few in numbers, there are still ongoing studies about the differentiation of OS subtypes and other primary bone tumor types based on the radiological findings [7, 8, 9].

In this study, we aimed to radiologically distinguish the osteoblastic type, which is the most common type of conventional OS, from the chondroblastic type, which is characterized by chondroid-looking immature tissues next to osteoid-forming areas, based upon X-ray findings and localizations and the quantitative values of intensity of the tumoral area detected with MRI imaging.

METHODS

This retrospective study was approved by the "Ethical Committee of the Faculty of Medicine, our institution," and is in compliance with the Helsinki Declaration (ID:2022/0403). Information on patients diagnosed with OS between January 2015 and March 2021 was retrieved from the database. Patients who

Received • Примљено: September 20, 2022
Revised • Ревизија: August 28, 2023
Accepted • Прихваћено: September 20, 2023
Online first: September 29, 2023

Correspondence to:
Sabriye GÜLÇIN BOZBEYOĞLU
Istanbul Goztepe Prof. Dr. Suleyman Yalcin City Hospital
Department of Radiology
Egitim Mahallesi Fahrettin Kerim Gokay Caddesi
34722 Kadıkoy/Istanbul
Turkey
gulcinbozbeyoglu@hotmail.com

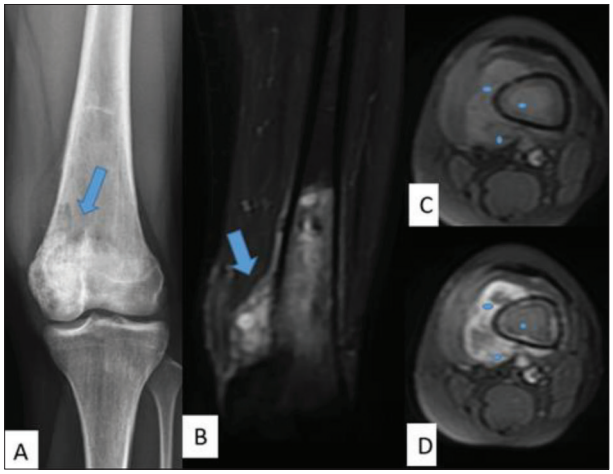

Figure 1. Osteoblastic osteosarcoma: A – anteroposterior radiograph shows a lytic sclerotic lesion of the distal femoral epiphysis-metaphysis (arrow); B – coronal T2 fast spin echo magnetic resonance image, distal femoral intramedullary tumor, and extraosseous extension (arrow); C – axial T1 fast spin echo magnetic resonance image; three dots indicate region of interest measurement sites; D – axial postcontrast T1 magnetic resonance image three region of interest marks placed in the same location

were operated on in our hospital, who had a pathologically confirmed diagnosis of OS, and had MRI scans were included in this study. Patients with secondary OS were not included. MRI scans with inadequate assessment quality as well as those that did not have fat-suppressed sequences and without contrast enhancement were excluded. Patients only diagnosed with osteoblastic or chondroblastic conventional subtypes were included in our study.

Direct radiographs of all patients were viewed from the picture archiving and communication system. Localization of lesions, Codman's and/or sunburst-type periosteal reactions, lytic and sclerotic features, the presence of calcification, and pathological fractures were investigated with X-rays.

Magnetic resonance imaging and measurement protocols

T1-weighted, T2-weighted, and contrast-enhanced T1-weighted images were obtained. For the contrast-enhanced studies, gadopentetate dimeglumine (0.1 mmol/kg body weight) was administered, and T1-weighted sequences with similar imaging parameters to the pre-contrast T1-weighted images were obtained.

T1-weighted spin-echo images were taken from the 1.5 Tesla MR device [field of view (FOV) 16, section thickness 4 mm, repetition time (TR) 426, echo time (TE) min], and T2 fast spin-echo images were taken from the 1.5 tesla MR device (FOV 16, section thickness 4 mm, TR 1500, TE 45).

These variations of TR, slice thickness, and FOV were changed depending on the number of slices and the size of the masses.

Lesions were grouped as femoral, tibial, and other according to their location in the bone. The diaphyseal, metaphyseal, and epiphyseal involvement sites in the bone were also noted (Table 1).

Table 1. Radiological findings of cases

Parameters	Group-1 (Osteoblastic) n = 14	Group-2 (Chondroblastic) n = 7	p value
Age (years)	25.5 ± 19.6	20.8 ± 11.3	0.573
Male	4 (28.6%)	4 (57.1%)	0.346
Female	10 (71.4%)	3 (42.9%)	
T1-ROI	636.3 ± 387.0	873.5 ± 610	0.288
T2-ROI	973.2 ± 525.7	981.5 ± 878.6	0.978
Contrast	1586.2 ± 945.7	1625.8 ± 1744.2	0.948
Localization			
Femur Tibia Other	6 (42.9%) 3 (21.4%) 5 (35.7%)	3 (42.9%) 3 (42.9%) 1 (14.3%)	0.599
Only D Only M D + M E + M E + M + D Other localization	4 (28.5%) 0 4 (28.5%) 1 (7.1%) 0 5 (35.6%)	2 (28.6%) 1 (14.3%) 2 (28.6%) 1 (14.3%) 1 (14.3%) 1 (14.3%)	0.499
Codman triangle	7 (%50)	2 (28.6%)	0.622
X-ray findings			
Sclerosis Pathological fracture Calcification Lytic lesion	5 (35.7%) 2 (14.2%) 1 (7.1%) 5 (35.7%)	3 (42.9%) 2 (28.6%) 0 1 (14.3%)	0.395
According to T1			
Hyperintense Hypointense Isointense Heterogenous	5 (35.7%) 4 (28.6%) 2 (28.6%) 3 (21.4%)	3 (42.9%) 3 (42.9%) - 1 (14.3%)	0.688
According to T2			
Hyperintense Hypointense	11 (78.6%) 3 (21.4%)	4 (57.1%) 3 (42.9%)	0.299

ROI – region of interest; D – diaphysis; M – metaphysis; E – epiphysis

Region of interest (ROI) was placed in three different areas of the tumors in enhanced sequences. While placing ROI, the areas with contrast enhancement were chosen and care was given not to involve-enhancing areas showing necrosis and cystic cavity. Then, the average ROI value was calculated for each sequence (Table 1).

Statistical analysis

Statistical analyses were performed using IBM SPSS Statistics for Windows, Version 20.0. (IBM Corp., Armonk, NY, USA). Normality testing was performed with the Kolmogorov–Smirnov test. Normal distributions were shown as mean ± standard deviation, non-normal distributions as median (interquartile range), and categorical variables as numbers and percentages. Differences between groups of numerical variables were evaluated with either the Student's t-test, or Mann–Whitney U-test according to normality distribution. Comparisons of categorical variables were performed using χ^2, Yates's correction, and Fisher's exact tests. The correlations between numerical variables were tested by the Spearman correlation analysis. Changes in cardiovascular magnetic resonance parameters were performed with paired sample t-tests, while differences between groups were by repeated measures of ANOVA analysis.

RESULTS

We retrospectively analyzed 21 patients with OS between 2015 and 2021. Osteoblastic OS was detected in 14 patients (66.6%). Chondroblastic OS was detected in seven patients (66.6%). In nine patients (42.8%), lesions were localized at the femur, and in six patients (28.5%) at the tibia. The sacrum was involved in three patients (14.2%), fibula in one patient (4.7%), and extraskeletal in two patients (9.5%).

All but three patients underwent resection of the tumor for diagnostic purposes. Patients were grouped according to their pathological subtypes. We found no correlation between X-ray findings and T1-ROI, T2-ROI, and their contrasts (Table 1).

The studied OS lesions showed heterogeneous signal patterns on different MRIs. Ossified matrices, although in variable proportions, were present in all lesions. X-ray evaluations of the osteoblastic OSs revealed pure lytic lesions in 35.7% and pure sclerotic lesions in 35.7%; other X-ray findings involved pathological fracture and calcifications. X-ray evaluations of the chondroblastic OSs revealed pure lytic lesions in 14.3% (Figure 2), pure sclerotic lesions in 42.9%, and pathological fractures in 28.6%. Of the chondroblastic OS lesions, 85.8%were located in the long bones. No statistically significant difference was detected according to the involvement sites in the bone (Table 1). There was no statistically significant difference in T1 and T2 signal intensities and fat-suppressed contrast-enhanced T1signal intensity between osteoblastic and chondroblastic types ($p = 0.288$, $p = 0.978$, and $p = 0.948$, respectively).

DISCUSSION

In this study we evaluated the correlation of OS subtypes with a pathological diagnosis with MR sequences conducted on 21 patients, no correlation was found between MR findings and OS subtypes.

Combining diagnostic imaging and a histopathological examination for the detection of bone tumors is indispensable [10]. Radiologically, OSs usually seem intense relative to muscle on T1-weighted images while hyperintense on T2-weighted images. Areas of low signal intensity are common in both T1-weighted and T2-weighted MR images and represent a mineralized matrix. In both intraosseous and soft tissue components, central hemorrhage foci appear hypointense on T1–T2 images; necrosis is hypointense on T1-weighted images and hyperintense on T2-weighted images. Variable imaging characteristics of rarer subtypes of OSs create diagnostic difficulties [11]. It may be possible with a combination of histopathological and radiological features to diagnose OS subtypes and manage appropriate treatment strategies, which have an important role in the survival of patients.

Conventional radiography is the first imaging procedure that provides a clue to the initial diagnosis, such as the aggressiveness of the tumor and hence prognosis. It also provides a differential diagnosis. Although the incidence of sclerotic lesions was higher in chondroblastic OS compared to osteoblastic sarcoma, this was not enough to produce a statistically significant value. However, the incidence of lytic lesions was higher in the osteoblastic sarcoma group compared to the chondroblastic OS group, but this did not reach a statistically significant value, probably owing to osteoid and chondroblastic matrix content heterogenicity. Bone lesions detected in radiography (the periosteal reaction, defined as Codman's triangle) were higher in osteoblastic OS, although not enough to reach a statistically significant value.

Although MRI modality may be superior in the staging of suspected or proven osteosarcomatous disease, as with other intraosseous lesions, it is the radiographic features of the tumor that are of primary importance in the generation of a specific diagnosis.

Conventional OSs are usually presented as intramedullary masses. Differentiating chondroblastic OS from other conventional OS types has clinical importance because of the differences in the prognosis [12]. Unfortunately, chondroblastic OSs are associated with a poor response to chemotherapy and display a high incidence of metastases. As chondroblastic OS are chemoresistant, the effect of a resection margin and the role of radical surgery is more important compared to osteoblastic OS for treatment and survival [13].

Due to the relatively low incidence of chondroblastic OS, cases describing its diagnosis and treatment strategies are extremely rare. The diagnosis of chondroblastic OS was made when the chondroid component involved at least 30% of the lesion, which is not always easy to detect. Non-enhanced T1-weighted magnetic resonance imaging (T1WI MRI) is an important preoperative examination used to visualize the intramedullary extent of malignant long bone tumors (Figures 2 and 3). Early reports showed that MRIs, especially T1WI MRIs in patients with primary bone tumors, were reliable for delineating lesion characteristics [14]. T1signal characteristics for the non-mineralized component is isointense, and for the mineralized/ossified component, it is hypointense. However, the T2 signal characteristics of the non-mineralized component are hyperintense, and the mineralized/ossified component is hypointense. No statistically significant difference was found between the T1 and T2 signal characteristics for osteoblastic and chondroblastic OSs. The potential additional value of Diffusion MRI imaging is to provide *in vivo* functional tissue information when it has been added to conventional MR to improve the specificity of lesion characterization. It is well understood that apparent diffusion coefficient (ADC) values reflect the pathological content of the tissues and the diffusion of water molecules in the extracellular space. Hence, it is expected in malignant tumors that high cellularity, pleomorphism, and hyperchromatism contribute to diffusion restriction [15, 16].

Diffusion-weighted (DW) MRI can be used to evaluate chemotherapy response in OS.

An increase in ADC is expected in assessing adequate treatment response [17]. Multiple studies have demonstrated the ability of DWI to differentiate between good and poor treatment responses in HG-OS. Wang et al. [17] assessed chemotherapy responses with DWI between different histological subtypes of HG-OS, identifying that

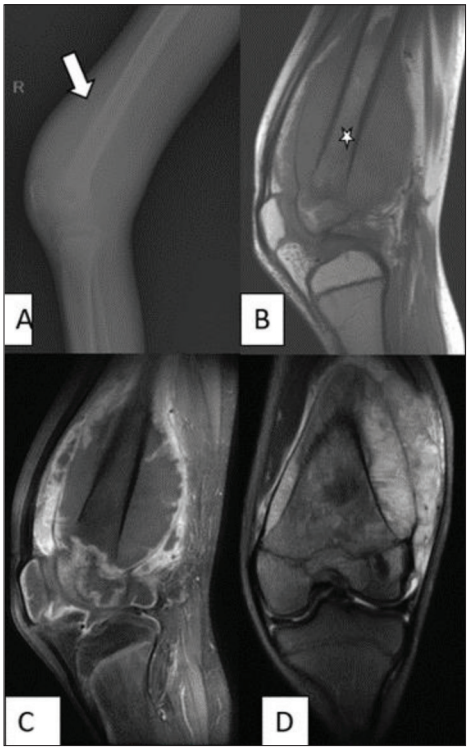

Figure 2. Chondroblastic osteosarcoma: A – lateral radiograph shows Codman triangle (arrow); B – sagittal T1-weighted fast spin echo magnetic resonance image of the femur intramedullary tumor extension diaphysis to epiphysis; C – postcontrast T1-weighted magnetic resonance imaging significant contrast enhancement; D – coronal T2-weighted fast spin echo magnetic resonance imaging extramedullary extension

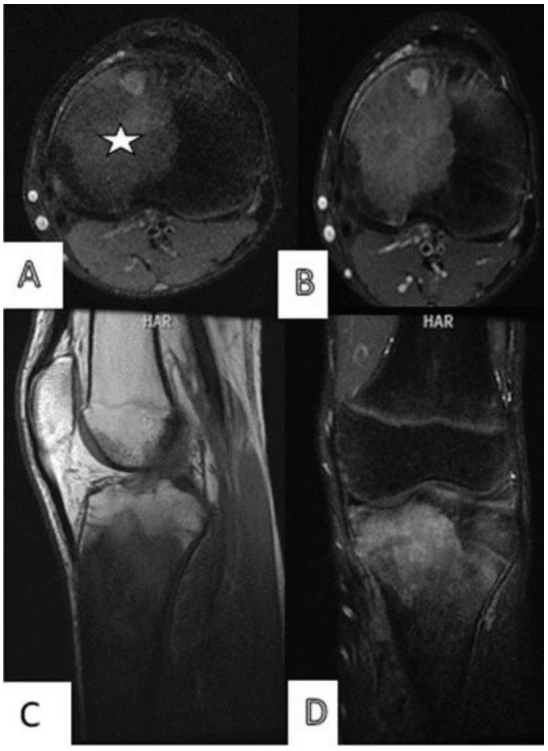

Figure 3. Chondroblastic osteosarcoma: A – axial T1-weighted fast spin echo magnetic resonance image of the tibia showing a lobular isointense morphology to the tumor (Stars); B – axial postcontrast T1-weighed magnetic resonance imaging displaying significant contrast enhancement; C – sagittal T1-weighted magnetic resonance imaging showing a lobular hypointense intramedullary component; D – hyperintense lesion extending to the epiphysis at coronal T2 weighted fast spin echo image

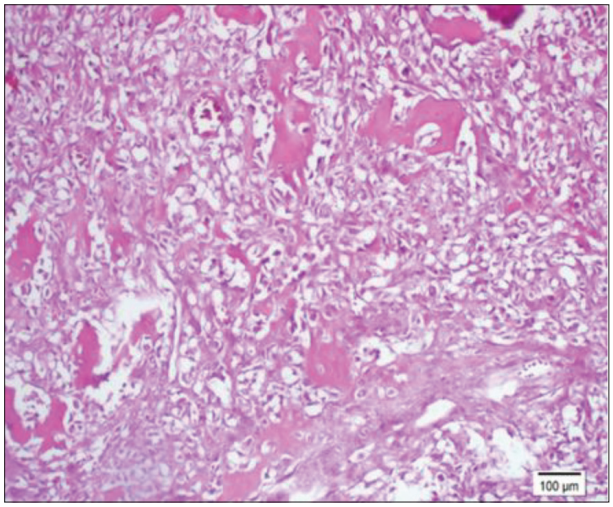

Figure 4. In osteoblastic osteosarcoma, the osteoid matrix is thin, reticulated, and lacy (Hematoxylin eosin × 100)

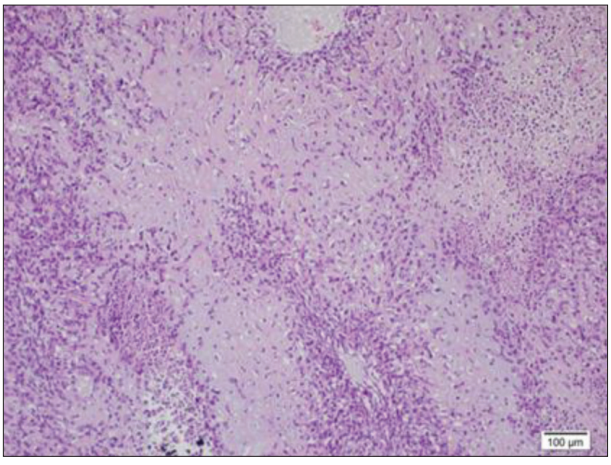

Figure 5. In chondroblastic osteosarcoma, the dominant component (usually 80–90%) is the chondroid, which is usually hyaline, less often myxoid cartilage matrix (Hematoxylin eosin × 100)

tumor necrosis could be differentiated from a viable tumor in fibroblastic and osteoblastic OS, but not in chondroblastic OS due to the inherently high ADC values of viable chondroblastic tissue [18].

In their studies, Pekcevik et al. [19] reported that chondrosarcomas had the highest ADC values among malignant bone tumors. Hayashida et al. [20] reported that there was no significant difference between the ADC values of solitary bone cysts, fibrous dysplasia, and chondrosarcomas with chondrosarcomas values lying in between the other two benign lesions. In another study, it was revealed significantly higher minimum ADC values of chondroblastic OS compared to other OS subtypes [8]. In our study, we could not involve DW MRI and ADC values because DW images (DWI) have only become standard after 2021.

Setiawati et al. [21] tried to analyze the histological subtypes of OS with dynamic contrast-enhanced MRI in addition to ADC characteristics. They found that osteoblastic OS had the highest value according to time intensity curve analysis and chondroblastic type OS had the highest value

according to ADC. They argued that in addition to determining the subtypes, the healing status of the disease and treatment response can be evaluated with this study [21].

Conventional OSs contain varying proportions of osteoblastic, chondroblastic, and fibroblastic areas. OS is classified as subtypes according to the matrix and dominant components. The variable histopathological structure of OS subtypes complicates the diagnosis. In OS, cells display marked pleomorphism and atypia. Neoplastic cells are in close association with the osteoid or chondroblastic matrix. In osteoblastic OS, the osteoid matrix is thin, reticulated, and lacy, and it has a yellowing appearance (Figure 4). In chondroblastic OS, the dominant component is usually the chondroid tissue (Figure 5). Chondroid areas are usually similar in grades 2–3 chondrosarcoma histology, and even a small amount of neoplastic osteoid formation should be present in chondroblastic OS. OS usually have mixed histology. ROI values in our study failed to distinguish between chondroblastic or osteoblastic types possibly due to mixed histological heterogeneity.

To our knowledge, this is the first study to differentiate conventional OSs involving osteoblastic and chondroblastic subtypes with quantitative T1, T2, and post-contrast signal intensity values by MRI. The main limitation of this study was having a small sample and studies with larger population should be planned in the future. Another limitation is that the study was conducted by a single observer.

CONCLUSION

Although no correlation was found between MRI parameters and histopathological findings in OS subtypes in the current study, it is promising to evaluate measurable parameters in MR sequences for prospective studies with larger patient groups to be conducted on this subject.

Conflict of interest: None declared.

REFERENCES

1. Grimer R, Athanasou N, Gerrand C, Judson I, Lewis I, Morland B, et al. UK Guidelines for the Management of Bone Sarcomas. Sarcoma. 2010;2010:317462. [DOI: 10.1155/2010/317462] [PMID: 21253474]
2. Casali PG, Bielack S, Abecassis N, Aro HT, Bauer S, Biagini R, et al. Bone sarcomas: ESMO-PaedCan-EURACAN Clinical Practice Guidelines for diagnosis, treatment, and follow-up. Ann Oncol. 2018;29(Suppl 4):iv79–iv95. [DOI: 10.1093/annonc/mdy310] [PMID: 30285218]
3. Misaghi A, Goldin A, Awad M, Kulidjian AA. Osteosarcoma: A comprehensive review. SICOT J. 2018;4:12. [DOI: 10.1051/sicotj/2017028] [PMID: 29629690]
4. He S, Jiang R, Sun H, Yang J, Ye C, Liu W, et al. Surgical efficacy and survival prediction of patients with unspecified malignant bone tumors. BMC Cancer. 2022;22(1):1078. [DOI: 10.1186/s12885-022-10153-x] [PMID: 36266614]
5. Nguyen JC, Baghdadi S, Pogoriler J, Guariento A, Rajapakse CS, Arkader A. Pediatric Osteosarcoma: Correlation of Imaging Findings with Histopathologic Features, Treatment, and Outcome. Radiographics. 2022;42(4):1196–213. [DOI: 10.1148/rg.210171] [PMID: 35594197]
6. Berkeley R, Andrei V, Saifuddin A. The rare primary bone sarcomas: imaging-pathological correlation. Skeletal Radiol. 2021;50(8):1491–511. [DOI: 10.1007/s00256-020-03692-6] [PMID: 33410967]
7. Zeitoun R, Shokry AM, Ahmed Khaleel S, Mogahed SM. Osteosarcoma subtypes: Magnetic resonance and quantitative diffusion weighted imaging criteria. J Egypt Natl Canc Inst. 2018;30(1):39–44. [DOI: 10.1016/j.jnci.2018.01.006] [PMID: 29429892]
8. Chianca V, Albano D, Messina C, Vincenzo G, Rizzo S, Del Grande F, et al. An update in musculoskeletal tumors: from quantitative imaging to radiomics. Radiol Med. 2021;126(8):1095–105. [DOI: 10.1007/s11547-021-01368-2] [PMID: 34009541]
9. Yen CH, Chang CY, Teng MM, Wu HT, Chen PC, Chiou HJ, et al. Different and identical features of chondroblastic osteosarcoma and chondrosarcoma: highlights on radiography and magnetic resonance imaging. J Chin Med Assoc. 2009;72(2):76–82. [DOI: 10.1016/S1726-4901(09)70027-9] [PMID: 19251535]
10. Campanacci M, Mercuri M, Gasbarrini A, Campanacci L. The value of imaging in the diagnosis and treatment of bone tumors. Eur J Radiol. 1998;27 Suppl 1:S116–22. [DOI: 10.1016/s0720-048x(98)00052-7] [PMID: 9652511]
11. Yarmish G, Klein MJ, Landa J, Lefkowitz RA, Hwang S. Imaging characteristics of primary osteosarcoma: Nonconventional subtypes. Radiographics. 2010;30(6):1653–72. [DOI: 10.1148/rg.306105524] [PMID: 21071381]
12. Bacci G, Bertoni F, Longhi A, Ferrari S, Forni C, Biagini R, et al. Neoadjuvant chemotherapy for high-grade central osteosarcoma of the extremity: Histologic response to preoperative chemotherapy correlates with histologic subtype of the tumor. Cancer. 2003;97(12):3068–75. [DOI: 10.1002/cancer.11456] [PMID: 12784343]
13. Hauben EI, Weeden S, Pringle J, Van Marck EA, Hogendoorn PCW. Does the histological subtype of high-grade central osteosarcoma influence the response to treatment with chemotherapy and does it affect overall survival? A study on 570 patients of two consecutive trials of the European Osteosarcoma Intergroup. Eur J Cancer. 2002;38(9):1218–25. [DOI: 10.1016/s0959-8049(02)00037-0] [PMID: 12044509]
14. Gulia A, Puri A, Subi TS, Gupta SM, Juvekar SL, Rekhi B. Comparison of MRI and Histopathology with regard to Intramedullary Extent of Disease in Bone Sarcomas. Sarcoma. 2019;2019:7385470. [DOI: 10.1155/2019/7385470] [PMID: 31885489]
15. Einarsdóttir H, Karlsson M, Wejde J, Bauer HCF. Diffusion-weighted MRI of soft tissue tumours. Eur Radiol. 2004;14(6):959–63. [DOI: 10.1007/s00330-004-2237-0] [PMID: 14767604]
16. Pretell-Mazzini J, Seldon CS, D'Amato G, Subhawong TK. Musculoskeletal Metastasis From Soft-tissue Sarcomas: A Review of the Literature. J Am Acad Orthop Surg. 2022;30(11):493–503. [DOI: 10.5435/JAAOS-D-21-00944] [PMID: 35320120]
17. Wang J, Sun M, Liu D, Hu X, Pui MH, Meng Q, et al. Correlation between apparent diffusion coefficient and histopathology subtypes of osteosarcoma after neoadjuvant chemotherapy. Acta Radiol. 2017;58(8):971–6. [DOI: 10.1177/0284185116678276] [PMID: 27852643]
18. Aoki T, Fujisaki A, Terasawa T, Hayashida Y, Todoroki Y, Hirano, et al. Primary Site Identification of Soft-Tissue Mass: Things to Know in MRI Assessment. J Magn Reson Imaging. 2022;55(1):37–47. [DOI: 10.1002/jmri.27368] [PMID: 32949073]
19. Pekcevik Y, Kahya M, Kaya A. Diffusion-weighted magnetic resonance imaging in the diagnosis of bone tumors: Preliminary results. J Clin Imaging Sci. 2013;3:63. [DOI: 10.4103/2156-7514.124094] [PMID: 24605258]
20. Hayashida Y, Hirai T, Yakushiji T, Katahira K, Shimomura O, Imuta M, et al. Evaluation of diffusion-weighted imaging for the differential diagnosis of poorly contrast-enhanced and T2-prolonged bone masses: Initial experience. J Magn Reson Imaging. 2006;23(3):377–82. [DOI: 10.1002/jmri.20512] [PMID: 16475145]
21. Setiawati R, Novariyanto B, Rahardjo P, Mustokoweni S, Guglielmi G. Characteristic of Apparent Diffusion Coefficient and Time Intensity Curve Analysis of Dynamic Contrast Enhanced MRI in Osteosarcoma Histopathologic Subtypes. Int J Med Sci. 2023;20(2):163–71. [DOI: 10.7150/ijms.77906] [PMID: 36794155]

Можемо ли разликовати конвенционалне подтипове остеосаркома (остеобластичне и хондробластичне) на основу интензитета магнетне резонанце

Сабје Гулчин Бозбејолу[1], Ајше Нур Токсоз Јилдирим[2]

[1]Градска болница Гозтепе „Проф. др Сулејман Јалчин", Одељење за радиологију, Истанбул, Турска;
[2]Градска болница Гозтепе „Проф. др Сулејман Јалчин", Одељење за патологију, Истанбул, Турска

САЖЕТАК

Увод/Циљ Остеосарком је најчешћи примарни малигни тумор костију код адолесцената и младих одраслих, са тенденцијом да производи различите количине остеоида, хрскавице и фиброзног матрикса.

Циљ овог истраживања је да се направи разлика између остеосаркомских подтипова, остеобластичних и хондробластичних, на основу налаза магнетне резонанце (МР) и рендгенског сигнала.

Методе Ретроспективна анализа је урађена за 21 патолошки доказан подтип остеосаркома: остеобластични ($n = 14$) и хондробластични ($n = 7$). Рендгенским снимком су испитана уобичајена коштана порекла, периосталне реакције, литичке и склеротичне карактеристике, присуство калцификације и патолошких прелома. Измерили смо средње вредности области интересовања за сваку лезију помоћу МРИ секвенце.

Резултати Међу лезијама остеосаркома, 57% је било локализовано на колену. Рендгенски прегледи остеобластичних остеосаркома су открили чисте литичке лезије у 35,7% и чисте склеротичне лезије у 42,9% случајева. Хондробластични остеосаркоми су открили чисте литичке лезије у 14,3% и чисте склеротичне лезије у 42,9% случајева. Због променљивих остеобластичних, хондробластичних и фибробластичних подручја и пропорција окошталог матрикса, лезије остеосаркома имају хетерогени МР сигнал. Међутим, није откривена статистички значајна вредност.

Закључак Према нашим резултатима, карактеристике МРИ сигнала и рендгенски налази можда неће моћи да разликују подтипове остеосаркома, тако да су неопходне проспективне студије са већим групама болесника.

Кључне речи: магнетна резонанца; остеосарком; подтип; област интересовања